Coupled Variability and Predictability in a Stochastic Climate Model of the Tropical Atlantic

FAMING WANG

Institute of Oceanology, Chinese Academy of Sciences, Qingdao, Shandong, China

PING CHANG

Department of Oceanography, Texas A&M University, College Station, Texas

(Manuscript received 12 October 2007, in final form 21 May 2008)

ABSTRACT

The coupled variability and predictability of the tropical Atlantic ocean–atmosphere system were analyzed within the framework of a linear stochastic climate model. Despite the existence of a meridional dipole as the leading mode, tropical Atlantic variability (TAV) is dominated by equatorial features and the subtropical variability is largely uncorrelated between the northern and southern Atlantic. This suggests that atmospheric stochastic forcing plays a dominant role in defining the spatial patterns of TAV, whereas the active air–sea feedbacks mainly enhance variability at interannual and decadal time scales, causing the spectra distinctive from the red spectrum. Under the stochastic forcing, the useful predictive skill for sea surface temperature measured by normalized error variance is limited to 2 months on average, which is 1 month longer than the predictive skill of damped persistence, indicating that the contribution of ocean dynamics and air–sea feedbacks is moderate in the tropical Atlantic. To achieve maximum predictability, processes such as ocean dynamics, thermodynamical and dynamical air–sea feedbacks, and the delicate mode–mode interactions should be correctly resolved in the coupled models. Therefore, predicting TAV poses more challenge than predicting El Niño in the tropical Pacific.

1. Introduction

Because of the small basin geometry, tropical Atlantic variability (TAV) is not dominated by a single mode like El Niño–Southern Oscillation (ENSO) in the tropical Pacific. Rather, it displays two modes of variability: a decadal meridional sea surface temperature (SST) gradient mode coupled with cross-equatorial wind anomalies and an interannual zonal SST mode coupled with along-equatorial wind anomalies (e.g., Servain 1991; Tanimoto and Xie 1999). These modes of variability affect the rainfall over adjacent land regions and thus are the subject of extensive studies in recent years (see Xie and Carton 2004, the references therein).

Analyses based on observations and model simulations have revealed that both internal air–sea interaction and external atmospheric influences contribute to TAV (Chang et al. 2006b). In principle, there are two main air–sea feedback processes operating within the tropical Atlantic sector. The first is the wind–evaporation–SST (WES) mechanism (Xie and Philander 1994), in which latent heat flux reinforces SST anomalies that feedback to the atmosphere and change the wind speed, causing further changes in the latent heat flux (Chang et al. 1997; Xie 1999). This heat flux–SST feedback is usually referred to as the thermodynamical coupling (feedback), because no ocean dynamic processes are involved. There is growing evidence suggesting that the thermodynamical feedback is responsible for the development of the meridional SST anomalies in the subtropics (e.g., Wagner 1996; Chang et al. 2000; Ruiz-Barradas et al. 2000; Chiang et al. 2002; Czaja et al. 2002; Kushnir et al. 2002; Frankignoul et al. 2004; Saravanan and Chang 2004; Hu and Huang 2006). The second is the dynamical coupling between zonal wind, equatorial SST, and subsurface thermal anomalies, operating in a similar fashion to the Bjerknes feedback in the Pacific ENSO (Zebiak 1993). The dynamical feedback, albeit weaker in strength, causes consid-

Corresponding author address: Faming Wang, Institute of Oceanology, Chinese Academy of Sciences, 7 Nanhai Rd., Qingdao, Shandong 266071, China.
E-mail: faming_wang@ms.qdio.ac.cn

DOI: 10.1175/2008JCLI2283.1

erable zonal SST anomalies in the eastern equatorial Atlantic (Carton and Huang 1994; Chang et al. 2000; Ruiz-Barradas et al. 2000; Sutton et al. 2000; Frankignoul et al. 2004; Huang et al. 2004; Okumura and Xie 2006; Keenlyside and Latif 2007). It is generally agreed that the dynamical and thermodynamical feedbacks, although positive in nature, are not able to support self-sustained oscillations in the tropical Atlantic, because the atmospheric and oceanic damping are strong (Frankignoul and Kestenare 2002; Frankignoul et al. 2004; Frankignoul and Kestenare 2005). Therefore, external forcing is needed to provide the background energy and drive TAV.

ENSO is the strongest climate signal on interannual time scales and can affect the tropical Atlantic through the atmospheric teleconnection (Nobre and Shukla 1996; Saravanan and Chang 2000; Giannini et al. 2001a,b; Mo and Häkkinen 2001; Chiang et al. 2002; Chikamoto and Tanimoto 2005; Chang et al. 2006a). The main feature of ENSO influence is the weakening of northeast trade winds during boreal winter and spring, which induces a positive latent heat anomaly, and in turn a warming event in the tropical Atlantic (Enfield and Mayer 1997; Sutton et al. 2000; Czaja et al. 2002). Chang et al. (2006a) also point out that the remote influence from ENSO can interact destructively with the dynamic feedback in the equatorial Atlantic, weakening the zonal mode variability. Another source of the external forcing is atmospheric weather noise, such as the North Atlantic Oscillation (NAO), arising from nonlinear instability processes intrinsic to the atmosphere and possessing little predictability on climate time scales (Watanabe and Kimoto 2000; Hurrell et al. 2003). In the North Atlantic, this noise forcing plays a central role in driving low-frequency variability of subtropical SST anomalies (Cayan 1992; Seager et al. 2000; Marshall et al. 2001; Wu et al. 2004). In the South Atlantic, the noise forcing may also induce SST anomalies by changing the strength of the subtropical high and the southeasterlies (Venegas et al. 1997; Trzaska et al. 2007).

Although both ENSO and atmospheric noise forcing contribute in defining the spatial patterns and temporal characteristics of the tropical Atlantic SST anomalies, they may play different roles in terms of predictability. For ENSO-related variability, the predictability is mainly determined by our ability to predict ENSO (Kushnir et al. 2006; Hu and Huang 2007), on which the regional air–sea interaction may even have a negative effect (Chang et al. 2006a). For non-ENSO-related variability, the predictability mainly comes from air–sea interactions and oceanic processes internal to the tropical Atlantic, because the external forcing is the unpredictable weather noise. In this study, we will only consider the non-ENSO-related variability and analyze its predictability within the framework of a linear stochastic climate model (Hasselmann 1976). In comparison with the fully coupled GCM studies (Stockdale et al. 2006; Hu and Huang 2007), the advantage of linear stochastic modeling is that its statistics of variability and predictability can be expressed in analytical form (see the appendix), which allows for a clear separation of the contributions of various predictable dynamics. Such linear stochastic models have been proven useful in revealing the predictability of a coupled ocean–atmosphere system (Thompson and Battisti 2000, 2001; Chang et al. 2004a,b).

The model used in this study is a linear intermediate coupled model developed by Wang and Chang (2008) for the stability analysis of the tropical Atlantic. It was shown that the model contains the following two leading coupled modes: a decadal meridional mode sustained by the thermodynamical feedback and an interannual zonal mode sustained by the dynamical feedback. For realistic coupling strength, however, the meridional mode interacts with the zonal mode destructively, which may cause the meridional mode to lose its oscillating nature as the dynamical feedback becomes sufficiently strong. Such a destructive interference between the coupled modes may present a challenge for predicting the tropical Atlantic variability. Exploration of the full predictability requires correct representations of both the dynamical and thermodynamical feedbacks as well as their subtle interactions, which will be demonstrated in this paper.

In the remaining sections herein, the linear intermediate coupled model is first introduced and the atmospheric stochastic forcing is derived in section 2. Then, the model is evaluated by comparing its simulation with the observation in section 3. Next, the predictability of the tropical Atlantic variability is explored and the predicable components are analyzed in section 4. Finally, the conclusions are drawn and the findings are highlighted in section 5.

2. A stochastic climate model of tropical Atlantic

The linear coupled model developed in Wang and Chang (2008) is of the form

$$\frac{d\mathbf{x}}{dt} = \mathbf{A}\mathbf{x} + \mathbf{f}, \tag{1}$$

where state variable $\mathbf{x}$ characterizes the SST, current, and thermocline depth anomalies; operator $\mathbf{A}$ denotes the coupled ocean–atmosphere dynamics and thermodynamics within the tropical Atlantic; external forcing $\mathbf{f}$ represents the influence of ENSO, NAO, and other

atmospheric disturbances. For realistic coupling strength **A** is stable, and (1) depicts a damped system driven by force **f**. Variability of such a system depends not only on the property of **A**, which is primarily controlled by the air–sea interaction internal to the tropical Atlantic (see Wang and Chang 2008, for a detailed analysis), but also on the characteristics of external forcing **f**, mainly the anomalous wind stress and the anomalous heat flux that are independent of the SST anomalies of the tropical Atlantic.

In principle, the atmospheric variables can be separated into two components, SST-related and non-SST-related, such that

$$\tau = \mu \mathcal{A} T + \zeta$$
$$Q = \nu \mathcal{B} T + \eta, \qquad (2)$$

where τ, Q, and T are wind stress, heat flux, and SST anomalies, respectively. The first terms on the rhs of (2), representing a linear atmospheric response to the local SST of the tropical Atlantic, are incorporated in **A** of (1) and are known as the SST–wind feedback $\mathcal{A}$ and SST–heat flux feedback $\mathcal{B}$, with coupling strength μ and ν, respectively. The second terms, ζ and η, are the external forcing **f** of (1), which may possibly be related to the SST anomalies outside of the tropical Atlantic. However, if both ζ and η are completely produced by atmospheric internal variability, then they can be treated as random disturbances, that is, white noise, on climate time scales. As a result, Eq. (1) becomes a stochastic climate model (Hasselmann 1976) with variability and predictability solved analytically in the appendix.

In this study, the structure of the air–sea feedbacks $\mathcal{A}$ and $\mathcal{B}$ and the pattern of the stochastic forcing **f** are empirically estimated from the 2° × 2° monthly fields of Comprehensive Ocean–Atmosphere Data Set (COADS) for 1950–90 (da Silva et al. 1994). First, a singular value decomposition (SVD) is performed on the 40-yr wind stress, heat flux, and SST anomalies, and the ocean–atmosphere feedbacks are constructed using the three leading SVD modes (Wang and Chang 2008). Then, the SST-related component is removed from the wind stress and heat flux in (2), and the residual (ζ, η), explaining 70% of the total variance, represents a 40-yr-long realization of the external forcing. Noting that the winds and the heat fluxes are not independent variables (e.g., the latent heat flux strongly depends on winds), we perform a combined EOF decomposition on (ζ, η) to identify the coherent pattern of stochastic forcing **f**. Next, the principal component (PC) time series are tested against the null hypothesis of white noise, using the Ljung–Box method (Ljung and Box 1978). Of the first 200 PC time series (96% of the residual variance), 20 time series (15% of the residual variance) fail the whiteness test at 95% confidence level. Presumably, those nonwhite time series represent the ENSO remote forcing, whose main influence in the tropical Atlantic is to enhance interannual variability rather than introduce new spatial modes (Huang 2004; Huang et al. 2004). As a convenient approximation, we keep all of the 200 EOFs in the following analysis and assume their PC time series to be independent white noise processes.[1] Consequently, the stochastic climate model (1) is designed to investigate the intrinsic ocean–atmosphere variability of the tropical Atlantic, whose predictability should be viewed as a low-limit estimate of the real system.

Numerically, the model domain covers the tropical Atlantic basin (from 20°S to ~20°N), the spatial resolution is 1° in latitude and 2° in longitude, and all of the computations were carried out by using two FORTRAN libraries: the Linear Algebra Package (LAPACK; Anderson et al. 2000) and the Subroutine Library in Control Theory (SLICOT; Benner et al. 1999).

3. Coupled variability under stochastic forcing

Previous studies of TAV have suggested that both the local air–sea coupling and the external atmospheric forcing affect the SST fluctuations, and their respective contributions are region dependent (Dommenget and Latif 2000; Ruiz-Barradas et al. 2000; Huang et al. 2004). To characterize the major coupled modes, we define the following four regions of variability: the northern tropical Atlantic (NTA), from 5° to 20°N; the southern tropical Atlantic (STA), from 5° to 20°S; the western equatorial Atlantic (WEA), from 3°S to 3°N and west of 20°W; and the eastern equatorial Atlantic (EEA), from 3°S to 3°N and east of 20°W. The regions are divided such that NTA and STA are the centers of action for the meridional mode (Wang and Chang 2008), and WEA and EEA are centers of action for the zonal mode (Keenlyside and Latif 2007). To facilitate the data–model comparison, the same analyses are applied to the 2° × 2° monthly extended reconstructed SST (ERSST) data of 1957–2007 (Smith and Reynolds 2003), as well as the model simulation of (1).

[1] When the stochastic forcing **f** is composed of only EOFs that pass the Ljung–Box test, the variability and predictability of model (1) is essentially the same, except for minor change in the variance distribution of SST anomalies in section 3.

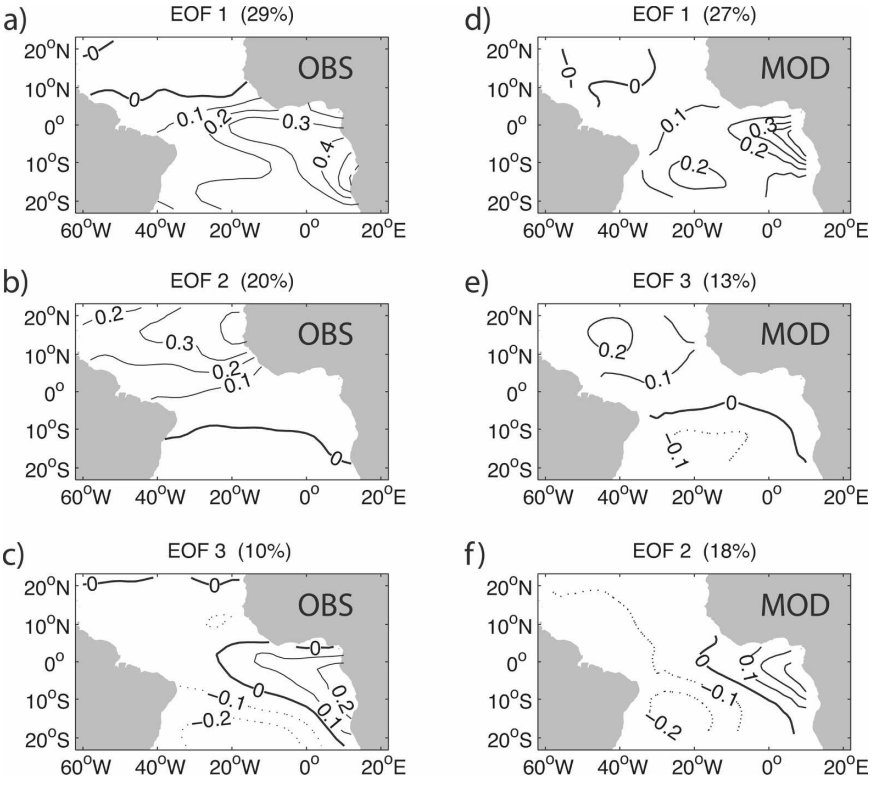

FIG. 1. Three leading EOFs of SST anomalies in the tropical Atlantic: (left) the observation, based on the 2° × 2° monthly ERSST data from 1957 to 2007 and (right) the model simulation, whose covariance matrix is computed analytically (see the appendix). The explained variance of each EOF is indicated in the parenthesis. The contour interval is 0.1°C. Note, the coupling strength is set to $\mu = 1.2$ and $\nu = 0.8$ in the stochastic model.

a. Observation

At each grid point of the tropical Atlantic, the climatology and trend were first removed to derive monthly ERSST anomalies $T(t)$, and then the ENSO influence was removed by subtracting an autoregressive process (Frankignoul and Sennéchael 2007)

$$Y(t) = \sum_{l=1}^{6} a_l N_1(t-l) + \sum_{l=1}^{6} b_l N_2(t-l)$$

from $T(t)$. While $N_1(t)$ and $N_2(t)$ are the first two PC time series of the Pacific SST anomalies between 12°N and 12°S, a and b are the autoregressive coefficients estimated through the Yule–Walker approach by assuming $T(t)$, a single realization of $Y(t)$. Additionally, $l = 1, \ldots, 6$ means that ENSO forcing takes about 6 months (at most) to affect TAV. The residual between $T(t)$ and $Y(t)$ is considered as the intrinsic tropical Atlantic variability, which was analyzed in the following.

Figures 1a–c show the patterns of the three leading EOFs of the ERSST observations, explaining 29%, 20%, and 10% of the variance, respectively. EOF-1 is characterized by coherent SST fluctuations in the south tropical Atlantic, with a maximal anomaly extending from the Angola coast to the central equatorial ocean. EOF-2 is characterized by coherent SST fluctuations in the north tropical Atlantic and a large meridional SST gradient across the equator. EOF-3, however, is characterized by the out-of-phase SST fluctuations between the northeast and southwest of the south tropical Atlantic. These are known patterns of TAV and have been investigated in various studies (Tanimoto and Xie 1999; Dommenget and Latif 2000; Ruiz-Barradas et al. 2000; Huang et al. 2004).

Apart from those coherent patterns in space, tropical Atlantic variability also exhibits coherence in time. Figure 2a shows that the three leading PC time series all have a red spectrum, superposed with some spectral peaks (not necessarily significant at the 95% confidence level). Generally speaking, EOF-1 has more power at interannual time scales, EOF-2 and EOF-3 have more power at decadal time scales. Cross correlations (Fig. 3a) further show that the tropical Atlantic displays considerable covariability between different regions, with

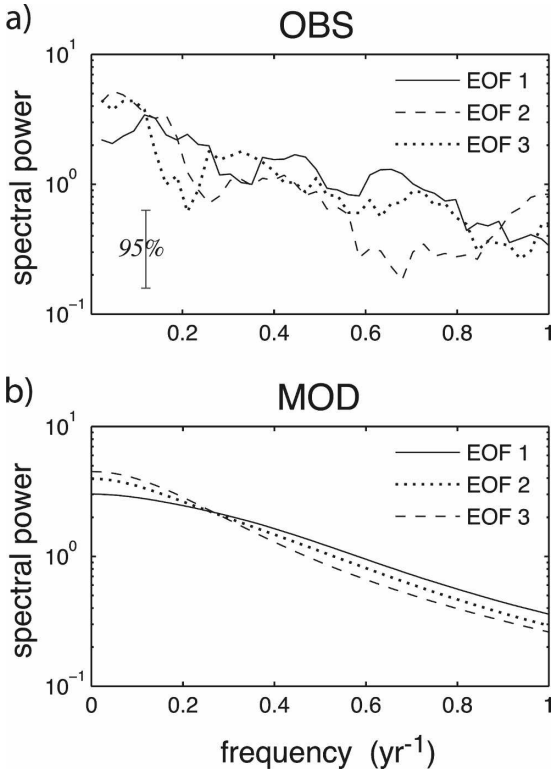

FIG. 2. Normalized power spectra of the PC time series of leading EOFs for the (a) 50-yr ERSST and (b) stochastic climate model. The spectra and 95% confidence interval in (a) are estimated via the multitaper method. The spectra in (b) are solved analytically via Eq. (A3) in the appendix, with the dotted line giving the best fit for a red spectrum $S(\omega) \propto 1/(\omega^2 + \lambda^2)$. Note, the coupling strength is set to $\mu = 1.2$ and $\nu = 0.8$ in the stochastic model.

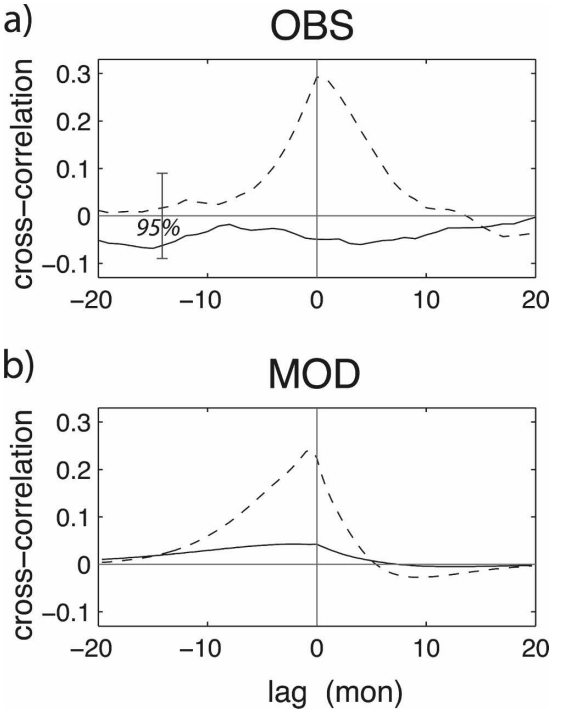

FIG. 3. Cross correlation of SST anomalies between the northern and southern tropical Atlantic (solid line) as well as the western and eastern equatorial Atlantic (dashed line) for the (a) 50-yr ERSST and (b) stochastic climate model. The 95% confidence interval is also calculated for the sampled correlations in (a). An estimation falling in this range implies that it is not significantly different from zero. The correlations in (b) are computed analytically (see the appendix), and hence there is no statistical sampling error. Note, the coupling strength is set to $\mu = 1.2$ and $\nu = 0.8$ in the stochastic model.

WEA and EEA showing the most significant cross correlation, and NTA and STA showing the most insignificant (not different from zero at 95% confidence). While the temporal coherence, a basis for the predictability of TAV, most likely is due to the regional air–sea feedbacks and ocean dynamics, the lack of correlation between NTA and STA, on the other hand, does not necessarily imply the absence of an interhemispheric coupled ocean–atmosphere mode in the tropical Atlantic (see section 3b).

b. Model simulation

Despite the fact that many processes, such as cloud and radiation feedbacks (Tanimoto and Xie 2002; Frankignoul and Kestenare 2002), are not included in (1), the simple stochastic model with realistic coupling strength is still capable of capturing the key features of TAV. For example, Figs. 1d–f and 2b show the modeled EOFs and the spectra of the associated PC time series for $\mu = 1.2$ and $\nu = 0.8$. In comparison with the observation, the interannual equatorial pattern (EOF-1), the decadal meridional pattern, and the subtropical dipole pattern in the south Atlantic are all reasonably well simulated, except that the second and third EOFs switch places between the observation and simulation. Furthermore, the high correlation between the western and eastern equatorial Atlantic and the lack of correlation between the northern and southern tropical Atlantic are also being reproduced by the model to a large extent (Fig. 3b).

The simplicity of the model enables us to investigate the effect of air–sea feedbacks on TAV. By varying the two coupling parameters, we found that the variance of EOF-1 increases as the dynamic feedback strengthens, while the variance of EOF-2 and EOF-3 increase as the thermodynamic feedback strengthens (not shown). This seems to suggest that EOF-1 has a dynamic origin, whereas EOF-2 and EOF-3 are more affected by the thermodynamic feedback. Although, in comparison with the stability analysis of Wang and Chang (2008),

the equatorial and subtropical variability may be viewed as manifestations of the dynamical and thermodynamical coupled modes, there are some fundamental differences. For example, while the least-damped mode of the tropical Atlantic coupled system is a decadal meridional oscillation (Wang and Chang 2008), the first EOF represents an interannual equatorial mode of variability (Fig. 1d). For realistic coupling strength, Wang and Chang (2008) show that the leading modes of TAV interfere with each other destructively, implying that the coupled system is nonnormal. Unlike a normal system with spatially independent forcing, in which the first EOF represents the first leading normal mode and the second EOF represents the second leading normal mode, the EOFs of a nonnormal system are jointly determined by the mode–mode interference as well as the spatial coherence of stochastic forcing (Chang et al. 2004a,b). Therefore, a one-to-one correspondence between the leading EOFs and the leading normal modes does not generally hold for TAV.

Another interesting observation is that even though the coupled model (1) contains a meridional dipole mode by construction (Wang and Chang 2008), the correlation between the variability of NTA and STA is very low (Fig. 3b). Presumably, the destructive modal interference could break the north–south connection of TAV, restricting the cross correlation (Wang and Chang 2008). To identify the cause, two additional experiments are carried out, the no-coupling case ($\mu = \nu = 0$ and a realistic forcing pattern), and the no-coherence case (realistic coupling strength and a spatially white-noise forcing). In both experiments, the correlation between NTA and STA is insignificant compared to the local persistence, implying that the independence of stochastic forcing is responsible for the low cross correlation observed in model (1). Nevertheless, the influence of the meridional mode is still visible, with positive correlation most likely when NTA leads STA, confirming the southward propagation of SST anomalies in the thermodynamical coupled mode (Wang and Chang 2008).

In summary, the key features of TAV are reasonably captured by the stochastic climate model under realistic coupling and stochastic forcing. It has yet to be demonstrated whether the deviation from the red spectrum observed in Fig. 2, representing the contribution of the active air–sea coupling, is important in terms of the predictable dynamics within the tropical Atlantic.

4. Predictable dynamics within tropical Atlantic

In this section, we investigate TAV predictability within the framework of linear stochastic modeling (see the appendix). The normalized error variance ϵ is used to measure the predictability. Because the system under consideration is linear, this is equivalent to measuring the percentage of predictable variance, which is $1 - \epsilon$ by definition. Taking $\epsilon \leq 0.5$ as a useful prediction skill, we further define a predictable time τ_o such that $\epsilon(\tau_o) = 0.5$, that is, leading time at which the error accounts for half of the total variance.

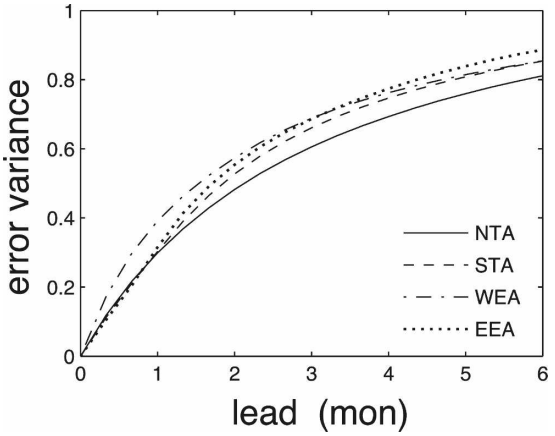

FIG. 4. Predictability of SST anomalies in the tropical Atlantic. Here, normalized error variance is used to measure the predictability of a stochastic system. As the lead time increases, the error grows and the system gradually loses predictability. Note, the coupling strength is set to $\mu = 1.2$ and $\nu = 0.8$ in the stochastic model.

a. Predictability of the tropical Atlantic variability

Figure 4 shows the predictability of SST anomalies in the four tropical Atlantic regions. In general, the predictable time is about 2 months for the tropical Atlantic SST. In detail, the subtropical variability is more predictable than the equatorial variability, with NTA being the most predictable and WEA being the least predictable. This is essentially consistent with the stability analysis of Wang and Chang (2008), that is, the meridional mode, which has the largest variability in NTA, dominates over the equatorial mode. As a result, the SST anomaly in NTA is less damped, and hence more persistent and predictable. While the low predictability of the equatorial SST anomaly basically reflects the fact that dynamical coupling in the equatorial Atlantic plays a much less dominant role than its counterpart in the equatorial Pacific, the western tropical Atlantic is further affected by the destructive interference of the coupled modes (Wang and Chang 2008), and hence is a less predictable region.

The area-averaged measure only provides general information about the spatial distribution of the predictability; a more detailed analysis is then carried out with

the aid of the so-called predictable component analysis, which was introduced by Schneider and Griffies (1999) and further developed by Chang et al. (2004a,b). Just like the principal component analysis in which the SST anomalies are decomposed into EOFs in terms of variance, here the SST anomalies are decomposed into a set of nonorthogonal patterns in terms of predictability. The pattern whose time series has maximal predictability is of special interest, named as the most predictable pattern. Figure 5 shows the most predictable pattern as well as the associated predictive skill for $\mu = 1.2$ and $\nu = 0.8$. As we can see, the most predictable pattern resembles the zonal mode and the meridional mode for short and long leads, respectively, while it displays both the zonal and meridional features for medium lead times. Another interpretation of the results in Fig. 5 is that the meridional and zonal modes possess different predictive skill and predictable time scales.

The transition from the zonal pattern to the meridional pattern as lead time increases can be easily understood within the linear stochastic framework. In the tropical Atlantic, the thermodynamical coupling dominates over the dynamical coupling; therefore, the meridional mode, rather than the zonal mode, becomes the least damped mode (Wang and Chang 2008). For short lead time, the most predictable pattern is closely linked to the leading EOF (Chang et al. 2004a,b), which in this case bears a resemblance to the zonal mode. For long lead time, the zonal mode and other high modes are asymptotically damped to zero; only the meridional mode can have an effect on predictability, and thus it shows up as the most predictable pattern. The relative strength of these two effects determines the most predictable pattern at medium lead times, which can be viewed as a hybrid of the two coupled modes.

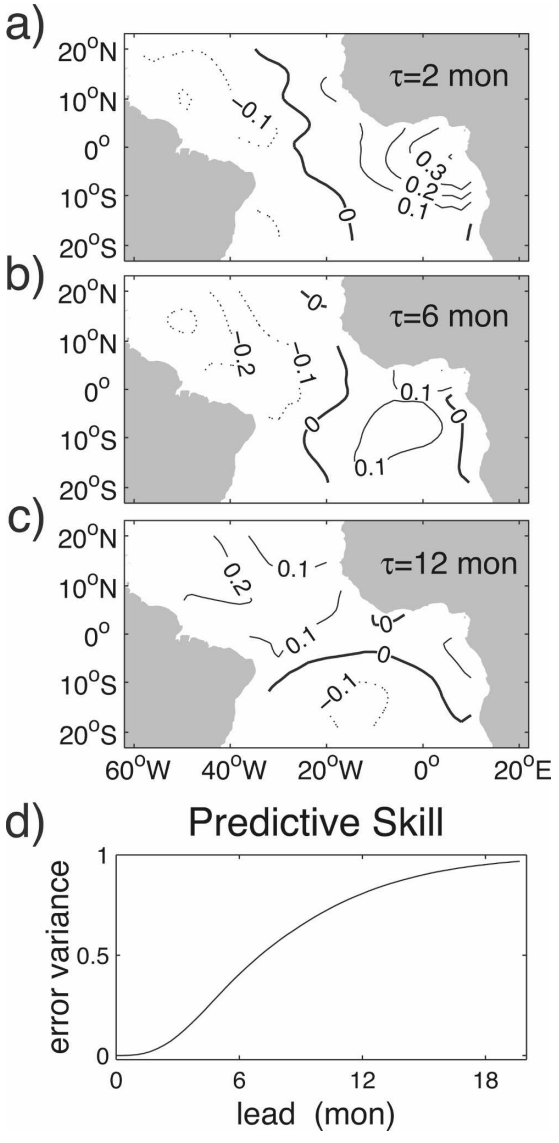

FIG. 5. (a)–(c) Most predictable pattern and (d) associated predictive skill as a function of lead time. For τ = (a) 2, (b) 6, and (c) 12 months, the most predictable pattern explains 22%, 15%, and 13% of total variance, respectively. Note, the coupling strength is set to $\mu = 1.2$ and $\nu = 0.8$ in the stochastic model.

b. Predictable dynamics in the coupled system

In the previous sections, we show that the regional air–sea couplings play crucial roles in shaping the variability and predictability of the tropical Atlantic SST. Here, we try to shed some light on the predictable dynamics of the tropical Atlantic by performing sets of "perfect" predictions. Assuming that the initial condition is precisely known, the prediction error is made up of the model error and the stochastic noise. The ideal case is that the model is perfectly accurate and that all of the prediction error is from noise forcing; we call this the optimal prediction and its skill is the system's predictability (see the appendix). If one of the physical processes is removed from the model, the prediction skill deviates from the predictability; the difference indicates how important the excluded process is in influencing the system's predictability.

The simplest prediction scheme is probably the persistence prediction, that is, that "tomorrow" has the same condition as "today." A prediction system is deemed useful only if it can beat the persistence. For the climate system, however, it is more appropriate for damped persistence to serve as the null hypothesis. In other words, assuming that the system is described by the 1D Hasselmann (1976) model, the future state would be the initial state damped at rate λ, such as

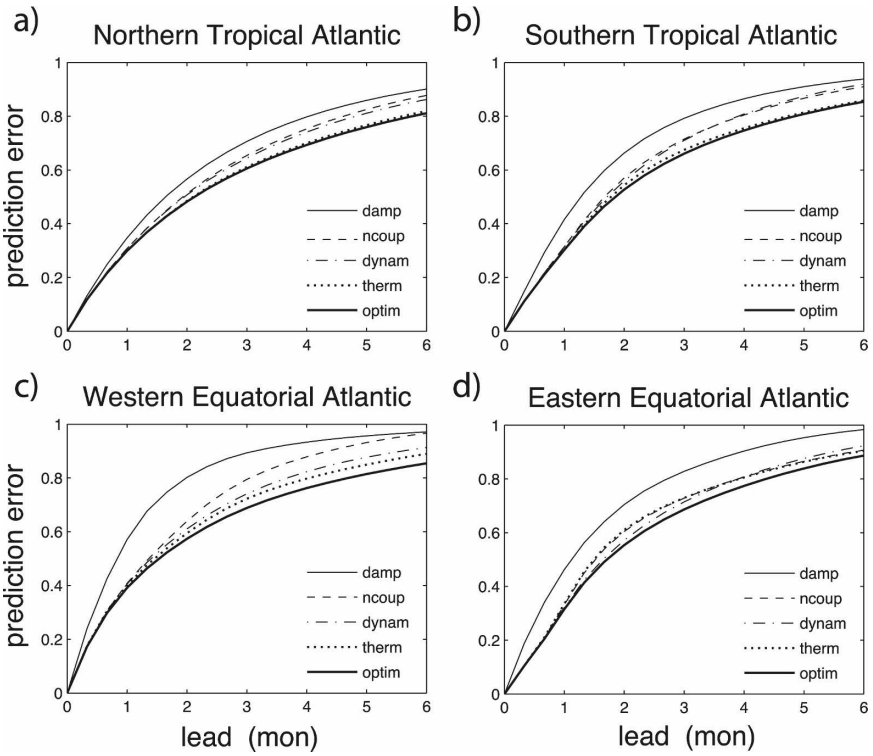

FIG. 6. Normalized prediction error of different prediction schemes for the (a) northern tropical Atlantic, (b) southern tropical Atlantic, (c) western equatorial Atlantic, and (d) eastern equatorial Atlantic. The skill of damped persistence prediction with $\lambda = 5$ months (thin solid line); the skill of prediction with no air–sea coupling in the model ($\mu = \nu = 0$), that is, the prediction model has ocean components only (dashed line); the skill of the prediction model with only dynamical coupling included ($\mu = 1.2$, $\nu = 0$; dash–dot line); the skill of prediction model with only thermodynamical coupling included ($\mu = 0$, $\nu = 0.8$; dotted line); and the skill of optimal prediction in which both dynamical and thermodynamical coupling are included ($\mu = 1.2$, $\nu = 0.8$; thick solid line). Presumably, the difference between the dashed line and the thin solid line denotes the contribution of ocean dynamics, the difference between the dash–dot line and the dashed line denotes the contribution of dynamical coupling, and the difference between the dotted line and the dashed line denotes the contribution of thermodynamical coupling. By definition, the thick solid line is the predictability illustrated in Fig. 4.

$x(\tau) = x(0)e^{-\lambda\tau}$. In the midlatitudes, where active air–sea interactions are very weak and SST fluctuates like red noise, much of the predictability can be explained by the damped persistence (Wang and Chang 2004). In the tropics, however, both the dynamical and thermodynamical couplings are active; therefore, the predictability of the tropical climate may be well above the skill of the damped persistence prediction. To explore the contribution of various coupling and oceanic processes, we carry out the following three additional predictions: one only includes the dynamical coupling, one only includes the thermodynamical coupling, and the third includes neither of the couplings.

The performance of different prediction schemes are compared in Fig. 6. As we expect, the prediction skill is bounded by the damped persistence and optimal prediction, because a prediction exceeding the predictability is impossible and being inferior to the damped persistence prediction is of little use. Beyond the damped persistence, the predictability of the tropical Atlantic SST anomalies has the following three components: the contribution from the thermodynamical air–sea feedback, mainly influencing the subtropical Atlantic; the contribution from the dynamical air–sea feedback, primarily affecting the equatorial Atlantic; and the contribution from the oceanic processes, mainly advection, which is important throughout the tropical Atlantic basin. Of special interest is the EEA region (Fig. 6d), where the dynamical feedback plays an important role in short lead time SST prediction, consistent with the previous findings (Chang et al. 2006a; Stockdale et al. 2006; Hu and Huang 2007).

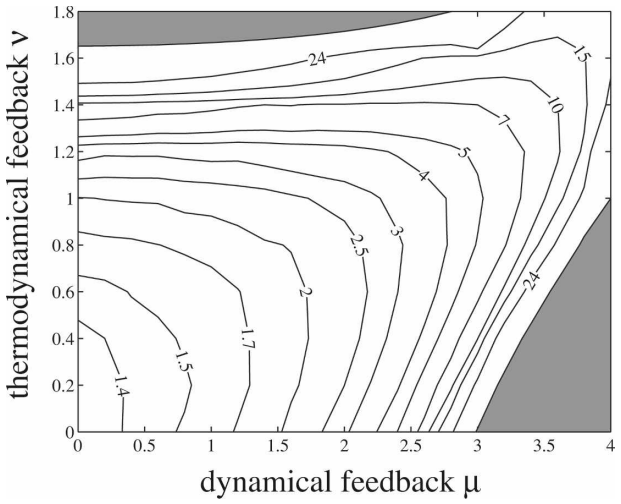

FIG. 7. Domain-averaged predictability of tropical Atlantic SST as a function of dynamical coupling strength μ and thermodynamical coupling strength ν. Shaded area delimits the unstable regime. Predictability is measured by the half-error time τ_o at which error and signal have equal variance, $\epsilon(\tau_o) = 0.5$.

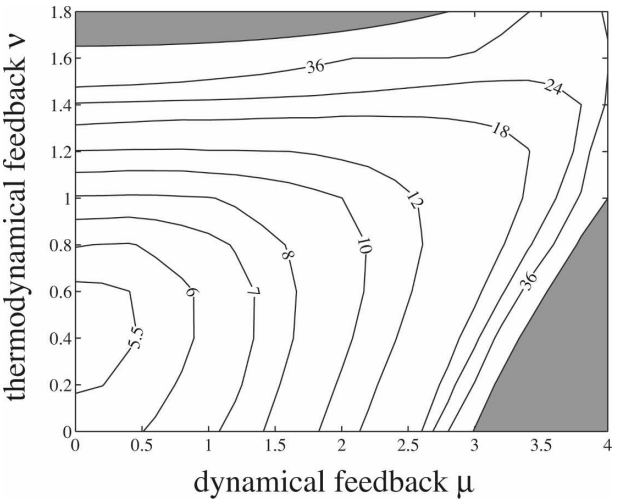

FIG. 8. Skill of the most predictable pattern as a function of dynamical coupling strength μ and thermodynamical coupling strength ν. Shaded area delimits the unstable regime. Skill is measured by the half-error time τ_o at which error and signal have equal variance, $\gamma(\tau_o) = 0.5$.

c. *Sensitivity to coupling strength*

Until now, both the dynamical and thermodynamical couplings are fixed at their realistic strengths ($\mu = 1.2$ and $\nu = 0.8$). In the tropical Atlantic, however, the SST anomalies are dominated by the meridional mode in boreal spring and the zonal mode in boreal summer, implying a seasonal shift in the coupling processes (Xie and Carton 2004; Chang et al. 2006b). Exploring the sensitivity of predictability to such a shift will tell us more about the predictable dynamics within the tropical Atlantic basin.

Figure 7 shows the predictable time of the total tropical Atlantic variability as a function of the coupling strength μ and ν. Generally, strong air–sea coupling, which is a destabilizing effect (Wang and Chang 2008), makes tropical Atlantic ocean–atmosphere more predictable. In fact, we can get an over- but still reasonable estimate of the predictable time just based on the damping rate of the meridional and zonal modes. This seems to suggest that much of the predictable dynamics within the tropical Atlantic is well captured by the two coupled modes. The overestimation results from neglecting the high damped modes as well as the destructive mode–mode interactions (Wang and Scott 2005). In the tropical Atlantic region, the modal interference is more important in strongly coupled cases, for example, an increase in the thermodynamical coupling from $\nu = 0$ for $\mu > 2$ indeed causes a decrease in the predictability.

Although the 2-month skill is probably not very impressive when predicting the variability of the entire tropical Atlantic, high predictability can still be achieved if only few spatial features are of interest. Figure 8 shows the skill, measured by the half-error time, of the most predictable pattern as a function of the coupling strength μ and ν. As we can see, the prediction time scale is about 6 months or longer. In comparison with the stability (Fig. 9 in Wang and Chang 2008), one immediately recognizes the striking similarity between the damping time scale of the first normal mode and the predictability of the most predictable pattern. In the thermodynamical regime, the predictability is determined by the heat flux–SST coupling with little influence from the dynamical feedback, and the most predictable pattern has the appearance of a meridional dipole (not shown). In the dynamical regime, the predictability is primarily defined by the wind stress–SST coupling, although some contribution from the thermodynamical feedback is also visible, and the most predictable pattern shows up as a zonal gradient pattern along equator (not shown). In the regime where both thermodynamical and dynamical feedbacks are strong and interfere with each other destructively, the most predictable pattern has mixed features of the meridional and zonal modes (like Fig. 5b).

5. Summary

A linear stochastic climate model of intermediate complexity is constructed to study TAV. The deterministic component includes the thermocline dynamics governed by the shallow-water equation, the Ekman dynamics and thermodynamics of the mixed layer, and

the positive air–sea feedbacks. The random component is introduced through the atmospheric stochastic forcing with spatial coherence derived from observations. With realistic coupling strength, the model reproduces the main features of the tropical Atlantic variability fairly well. The first three EOFs, explaining 60% of the variance in total, delineate the tropical Atlantic variability into the equatorial pattern that has enhanced power at interannual time scales, the meridional dipole pattern that has enhanced power at decadal time scales, and the south subtropical pattern that has a largely red spectrum. The regional air–sea feedbacks are the key factors for the tropical Atlantic to maintain interannual–decadal variability above a red spectrum. Because the tropical Atlantic ocean–atmosphere system is highly damped, the atmospheric stochastic forcing has crucial roles to play in determining the spatial and temporal characteristics of TAV. For example, despite the existence of a distinct meridional mode in the model, variability of the northern and southern tropical Atlantic are uncorrelated, just like the observation. The absence of correlation mainly results from the independence of stochastic forcing between the North and South Atlantic. Identifying the sources of the atmospheric stochastic forcing and the mechanisms by which the remote forcing reach the tropical Atlantic, however, is a challenging task and beyond the scope of this paper.

With the tools recently developed for analyzing the predictability of linear stochastic systems (Schneider and Griffies 1999; Chang et al. 2004a,b), we further investigate the predictable dynamics in the tropical Atlantic sector. On average, the tropical Atlantic SST has a 2-month predictability, with NTA the most predictable and WEA the least predictable. Among that, more than half of the predictability is accounted for by the damped persistence, which corresponds to the forced tropical Atlantic variability that is captured by an AGCM coupled to a slab ocean model (Trzaska et al. 2007). The second contribution to the predictability then comes from the ocean dynamics, namely, advection, entrainment, and thermocline perturbations. For instance, the mean advection could shift the signal downstream and redistribute the predictability (Wang and Chang 2004). This contribution corresponds to additional forced variability of the tropical Atlantic SST that is captured by a dynamic ocean model. Finally, the remaining predictability is explained by the regional air–sea feedbacks in the tropical Atlantic. In NTA and STA, the thermodynamical feedback predominates over the dynamical feedback, providing most of the predictability for coupled SST anomalies. Of special interest, however, is the equatorial Atlantic, where the dynamical feedback between winds and SST prevails. There, the thermodynamical feedback can take effect in two ways—affecting the SST anomalies directly (WEA) and interfering with the dynamical feedback destructively (EEA). To fully explore the potential predictability, both the oceanic processes and the air–sea feedbacks (thermodynamic, dynamic, as well as their interference) need to be correctly resolved in the coupled models. Therefore, the SST anomalies in the tropical Atlantic, especially the equatorial regions, prove to be difficult to predict (Chang et al. 2006a; Stockdale et al. 2006).

In conclusion, we demonstrated that much of the coupled variability and predictability of tropical Atlantic SST anomalies are linked to dominant coupled modes (the meridional mode and the zonal mode) and their destructive interaction under stochastic forcing. It should be made clear, however, that the predictability estimate presented in this study merely serves as a null hypothesis for the intrinsic variability of the tropical Atlantic. The ENSO influence, an important trigger and driving force of the tropical Atlantic variability, might provide additional predictability at interannual time scales, thus nullifying the hypothesis (Hu and Huang 2007).

Acknowledgments. The three anonymous reviewers are acknowledged for their constructive comments on the manuscript. This paper grows out of FW's Ph.D. dissertation research, which was partially supported by the National Science Foundation Grant ATM-9907625. FW is supported by the National Natural Science Foundation of China (Grant 40776015), the National Basic Research Program of China (973 Program Grants 2006CB403603 and 2007CB411802), and the Hundred Talents Program of the Chinese Academy of Sciences. PC is supported by the National Science Foundation Grants ATM-0337846 and OCE-0623364 and the National Oceanic and Atmospheric Administration (NOAA) Climate Program Grant NA050AR4311136.

APPENDIX

Predictability of a Linear Stochastic Model

For the stochastic climate system

$$\frac{d\mathbf{x}}{dt} = \mathbf{A}\mathbf{x} + \boldsymbol{\eta}, \tag{A1}$$

with linear stable operator $\mathbf{A}$ and normally distributed white noise $\boldsymbol{\eta} \sim \mathcal{N}(0, \boldsymbol{\Sigma})$, its solution

$$\mathbf{x}(t_0 + \tau) = e^{\mathbf{A}\tau}\mathbf{x}(t_0) + \int_0^{\tau} e^{\mathbf{A}(\tau - s)}\boldsymbol{\eta}(s + t_0)\, ds \tag{A2}$$

is composed of the following two components: the first term on the rhs represents the growth of the initial condition, and hence the predictable component $\mathbf{x}_s$; the second term on the rhs, independent of the first, represents the influence of random noise forcing, and hence the unpredictable component $\mathbf{x}_n$.

The covariance matrix $\mathbf{C} = \langle \mathbf{x}(t)\mathbf{x}^{\mathrm{T}}(t)\rangle$ and autocovariance matrix $\mathbf{C}_\tau = \langle \mathbf{x}(t+\tau)\mathbf{x}^{\mathrm{T}}(t)\rangle$ are given by the Lyapunov equation $\mathbf{AC} + \mathbf{CA}^{\mathrm{T}} = -\mathbf{\Sigma}$ and relation $\mathbf{C}_\tau = e^{\mathbf{A}\tau}\mathbf{C}$, respectively. Furthermore, the Fourier transform of (A1) gives the cross-spectrum matrix

$$\mathbf{S}(\omega) = (i\omega\mathbf{I} - \mathbf{A})^{-1}\mathbf{\Sigma}(i\omega\mathbf{I} - \mathbf{A})^{-\dagger}, \tag{A3}$$

where $\mathbf{I}$ is the unitary matrix and $(\cdot)^{-\dagger}$ denotes the conjugate transpose of matrix inverse.

For an arbitrary prediction $\mathbf{x}_p(t_0 + \tau) = f(\mathbf{x}(t_0), \tau)$, the prediction error is $\mathbf{x}_e = \mathbf{x}_s - \mathbf{x}_p + \mathbf{x}_n$ and the normalized error variance is

$$\epsilon(\tau) = \frac{\langle \mathbf{x}_e^{\mathrm{T}}\mathbf{x}_e\rangle}{\langle \mathbf{x}^{\mathrm{T}}\mathbf{x}\rangle} = 1 + \frac{\langle \mathbf{x}_p^{\mathrm{T}}\mathbf{x}_p\rangle}{\mathrm{tr}(\mathbf{C})} - 2\frac{\langle \mathbf{x}_s^{\mathrm{T}}\mathbf{x}_p\rangle}{\mathrm{tr}(\mathbf{C})}. \tag{A4}$$

Then, one can easily show that the error variance of the persistence prediction $\mathbf{x}(t_0 + \tau) = \mathbf{x}(t_0)$ is

$$\epsilon_p(\tau) = 2[1 - \rho(\tau)], \tag{A5}$$

with the autocorrelation

$$\rho(\tau) = \frac{\langle \mathbf{x}^{\mathrm{T}}(t_0+\tau)\mathbf{x}(t_0)\rangle}{\langle \mathbf{x}^{\mathrm{T}}\mathbf{x}\rangle} = \frac{\mathrm{tr}(\mathbf{C}_\tau)}{\mathrm{tr}(\mathbf{C})}; \tag{A6}$$

the error variance of damped persistence prediction $\mathbf{x}_p(t_0 + \tau) = e^{-\lambda\tau}\mathbf{x}(t_0)$ is

$$\epsilon_d(\tau) = 1 + e^{-2\lambda\tau} - 2e^{-\lambda\tau}\rho(\tau), \tag{A7}$$

with damping time scale of $\lambda^{-1} \approx 5$ months in the tropical Atlantic; and the error variance of optimal prediction $\mathbf{x}_p(t_0 + \tau) = \mathbf{x}_s = e^{\mathbf{A}\tau}\mathbf{x}(t_0)$ is

$$\epsilon_o(\tau) = 1 - \frac{\mathrm{tr}[e^{\mathbf{A}\tau}\mathbf{C}e^{\mathbf{A}^{\mathrm{T}}\tau}]}{\mathrm{tr}(\mathbf{C})}. \tag{A8}$$

Note, $\epsilon_o = \min\epsilon$ is an inherent property of (A1); it serves as a measure of the predictability in a global average sense. To study spatial variations, one can decompose the system (A1) into a series of spatial patterns

$$\mathbf{x}(t) = \sum \alpha_i(t)\mathbf{v}_i \tag{A9}$$

such that the predictability of time series $\alpha_i(t)$ are maximized. The pattern with maximum predictability is called the most predictable pattern, which is found through a generalized eigenvalue problem

$$e^{\mathbf{A}\tau}\mathbf{C}e^{\mathbf{A}^{\mathrm{T}}\tau}\mathbf{u} = \gamma\mathbf{C}\mathbf{u}, \tag{A10}$$

with $\mathbf{u}$ and $\mathbf{v}$ forming a biorthogonal set. For small τ, we may substitute the Taylor expansion of matrix exponential

$$e^{\mathbf{A}\tau} = \mathbf{I} + \mathbf{A}\tau + \cdots \tag{A11}$$

into the lhs of (A 10), and obtain an equivalent eigenvalue problem

$$(1 - \gamma)\mathbf{C}\mathbf{u} = \tau\mathbf{\Sigma}\mathbf{u}. \tag{A12}$$

Equation (A12) basically says that for short lead times the predictable component is strongly influenced by the forcing pattern. For more information on the prediction and predictability of linear stochastic systems, see Chang et al. (2004a,b) and Wang and Scott (2005).

REFERENCES

Anderson, E., and Coauthors, 2000: *LAPACK Users' Guide.* 3d ed. SIAM, 407 pp.

Benner, P., V. Mehrmann, V. Sima, S. Van Huffel, and A. Varga, 1999: SLICOT—A subroutine library in systems and control theory. *Applied and Computational Control, Signals and Circuits,* B. N. Datta, Ed., Springer-Verlag, 499–539.

Carton, J. A., and B. Huang, 1994: Warm events in the tropical Atlantic. *J. Phys. Oceanogr.,* **24,** 888–903.

Cayan, D. R., 1992: Latent and sensible heat flux anomalies over the northern oceans: Driving the sea surface temperature. *J. Phys. Oceanogr.,* **22,** 859–881.

Chang, P., L. Ji, and H. Li, 1997: A decadal climate variation in the tropical Atlantic Ocean from thermodynamic air-sea interactions. *Nature,* **385,** 516–518.

——, R. Saravanan, L. Ji, and G. C. Hegerl, 2000: The effect of local sea surface temperatures on atmospheric circulation over the tropical Atlantic sector. *J. Climate,* **13,** 2195–2216.

——, ——, T. DelSole, and F. Wang, 2004a: Predictability of linear coupled systems. Part I: Theoretical analysis. *J. Climate,* **17,** 1474–1486.

——, ——, F. Wang, and L. Ji, 2004b: Predictability of linear coupled systems. Part II: An application to a simple model of tropical Atlantic variability. *J. Climate,* **17,** 1487–1503.

——, Y. Fang, R. Saravanan, L. Ji, and H. Seidel, 2006a: The cause of the fragile relationship between the Pacific El Niño and the Atlantic Niño. *Nature,* **443,** 324–328, doi:10.1038/nature05053.

——, and Coauthors, 2006b: Climate fluctuations of tropical coupled systems—The role of ocean dynamics. *J. Climate,* **19,** 5122–5174.

Chiang, J. C. H., Y. Kushnir, and A. Giannini, 2002: Deconstructing Atlantic Intertropical Convergence Zone variability: Influence of the local cross-equatorial sea surface temperature gradient and remote forcing from the eastern equatorial Pacific. *J. Geophys. Res.,* **107,** 4004, doi:10.1029/2000JD000307.

Chikamoto, Y., and Y. Tanimoto, 2005: Role of specific humidity anomalies in Caribbean SST response to ENSO. *J. Meteor. Soc. Japan,* **83,** 959–975.

Czaja, A., P. van der Vaart, and J. Marshall, 2002: A diagnostic

study of the role of remote forcing in tropical Atlantic variability. *J. Climate,* **15,** 3280–3290.

da Silva, A. M., A. C. Young, and S. Levitus, 1994: *Algorithms and Procedures.* Vol. 1, *Atlas of Surface Marine Data 1994,* NOAA Atlas NESDIS 6, 83 pp.

Dommenget, D., and M. Latif, 2000: Interannual to decadal variability in the tropical Atlantic. *J. Climate,* **13,** 777–792.

Enfield, D. B., and D. A. Mayer, 1997: Tropical Atlantic sea surface temperature variability and its relation to El Niño Southern Oscillation. *J. Geophys. Res.,* **102,** 929–945.

Frankignoul, C., and E. Kestenare, 2002: The surface heat flux feedback. Part I: Estimates from observations in the Atlantic and the North Pacific. *Climate Dyn.,* **19,** 633–647.

——, and ——, 2005: Air–sea interactions in the tropical Atlantic: A view based on lagged rotated maximum covariance analysis. *J. Climate,* **18,** 3874–3890.

——, and N. Sennéchael, 2007: Observed influence of North Pacific SST anomalies on the atmospheric circulation. *J. Climate,* **20,** 592–606.

——, E. Kestenare, M. Botzet, A. F. Carril, H. Drange, A. Pardaens, L. Terray, and R. Sutton, 2004: An intercomparison between the surface heat flux feedback in five coupled models, COADS and the NCEP reanalysis. *Climate Dyn.,* **22,** 373–388, doi:10.1007/s00382-003-0388-3.

Giannini, A., M. A. Cane, and Y. Kushnir, 2001a: Interdecadal changes in the ENSO teleconnection to the Caribbean region and the North Atlantic oscillation. *J. Climate,* **14,** 2867–2879.

——, J. C. H. Chiang, M. A. Cane, Y. Kushnir, and R. Seager, 2001b: The ENSO teleconnection to the tropical Atlantic Ocean: Contributions of the remote and local SSTs to rainfall variability in the tropical Americas. *J. Climate,* **14,** 4530–4544.

Hasselmann, K., 1976: Stochastic climate models: Part I. Theory. *Tellus,* **28,** 473–485.

Hu, Z.-Z., and B. Huang, 2006: Physical processes associated with the tropical Atlantic SST meridional gradient. *J. Climate,* **19,** 5500–5518.

——, and ——, 2007: The predictive skill and the most predictable pattern in the tropical Atlantic: The effect of ENSO. *Mon. Wea. Rev.,* **135,** 1786–1806.

Huang, B., 2004: Remotely forced variability in the tropical Atlantic Ocean. *Climate Dyn.,* **23,** 133–152, doi:10.1007/s00382-004-0443-8.

——, P. S. Schopf, and J. Shukla, 2004: Intrinsic ocean–atmosphere variability of the tropical Atlantic Ocean. *J. Climate,* **17,** 2058–2077.

Hurrell, J. W., Y. Kushnir, G. Ottersen, and M. Visbeck, Eds., 2003: *The North Atlantic Oscillation: Climate Significance and Environmental Impact. Geophys. Monogr.,* Vol. 134, Amer. Geophys. Union, 279 pp.

Keenlyside, N. S., and M. Latif, 2007: Understanding equatorial Atlantic interannual variability. *J. Climate,* **20,** 131–142.

Kushnir, Y., R. Seager, J. Miller, and J. C. Chiang, 2002: A simple coupled model of tropical Atlantic decadal climate variability. *Geophys. Res. Lett.,* **29,** 2133, doi:10.1029/2002GL015874.

——, W. A. Robinson, P. Chang, and A. W. Robertson, 2006: The physical basis for predicting Atlantic sector seasonal-to-interannual climate variability. *J. Climate,* **19,** 5949–5970.

Ljung, G. M., and G. E. P. Box, 1978: On a measure of lack of fit in time series models. *Biometrika,* **65,** 297–303.

Marshall, J., and Coauthors, 2001: North Atlantic climate variability: Phenomena, impacts and mechanisms. *Int. J. Climatol.,* **21,** 1863–1898.

Mo, K. C., and S. Häkkinen, 2001: Interannual variability in the tropical Atlantic and linkages to the Pacific. *J. Climate,* **14,** 2740–2762.

Nobre, P., and J. Shukla, 1996: Variations of sea surface temperature, wind stress, and rainfall over the tropical Atlantic and South America. *J. Climate,* **10,** 2464–2479.

Okumura, Y., and S.-P. Xie, 2006: Some overlooked features of tropical Atlantic climate leading to a new Niño-like phenomenon. *J. Climate,* **19,** 5859–5874.

Ruiz-Barradas, A., J. A. Carton, and S. Nigam, 2000: Structure of interannual-to-decadal climate variability in the tropical Atlantic sector. *J. Climate,* **13,** 3285–3297.

Saravanan, R., and P. Chang, 2000: Interaction between tropical Atlantic variability and El Niño–Southern Oscillation. *J. Climate,* **13,** 2177–2194.

——, and ——, 2004: Thermodynamic coupling and predictability of tropical sea surface temperature. *Earth Climate: The Ocean-Atmosphere Interactions, Geophys. Monogr.,* Vol. 147, Amer. Geophys. Union, 171–180.

Schneider, T., and S. M. Griffies, 1999: A conceptual framework for predictability studies. *J. Climate,* **12,** 3133–3155.

Seager, R., Y. Kushnir, M. Visbeck, N. Naik, J. Miller, G. Krahmann, and H. Gullen, 2000: Cause of Atlantic Ocean climate variability between 1958 and 1998. *J. Climate,* **13,** 2845–2862.

Servain, J., 1991: Simple climatic indicies for the tropical Atlantic Ocean and some applications. *J. Geophys. Res.,* **96** (C8), 15 137–15 146.

Smith, T. M., and R. W. Reynolds, 2003: Extended reconstruction of global sea surface temperatures based on COADS data (1854–1997). *J. Climate,* **16,** 1495–1510.

Stockdale, T. N., M. A. Balmaseda, and A. Vidard, 2006: Tropical Atlantic SST prediction with coupled ocean–atmosphere GCMs. *J. Climate,* **19,** 6047–6061.

Sutton, R. T., S. P. Jewson, and D. P. Rowell, 2000: The elements of climate variability in the tropical Atlantic region. *J. Climate,* **13,** 3261–3284.

Tanimoto, Y., and S.-P. Xie, 1999: Ocean-atmosphere variability over the pan-Atlantic basin. *J. Meteor. Soc. Japan,* **77,** 31–46.

——, and ——, 2002: Inter-hemispheric decadal variations in SST, surface wind, heat flux and cloud cover over the Atlantic Ocean. *J. Meteor. Soc. Japan,* **80,** 1199–1219.

Thompson, C. J., and D. S. Battisti, 2000: A linear stochastic dynamical model of ENSO. Part I: Model development. *J. Climate,* **13,** 2818–2832.

——, and ——, 2001: A linear stochastic dynamical model of ENSO. Part II: Analysis. *J. Climate,* **14,** 445–466.

Trzaska, S., A. W. Robertson, J. D. Farrara, and C. R. Mechoso, 2007: South Atlantic variability arising from air–sea coupling: Local mechanisms and tropical–subtropical interactions. *J. Climate,* **20,** 3345–3365.

Venegas, S. A., L. A. Mysak, and D. N. Straub, 1997: Atmosphere–ocean coupled variability in the South Atlantic. *J. Climate,* **10,** 2904–2920.

Wagner, R. G., 1996: Mechanisms controlling variability of the interhemispheric sea surface temperature gradient in the tropical Atlantic. *J. Climate,* **9,** 2010–2019.

Wang, F., and P. Chang, 2004: Effect of oceanic advection on the potential predictability of sea surface temperature. *J. Climate,* **17,** 3603–3615.

——, and R. Scott, 2005: On the prediction of linear stochastic systems with a low-order model. *Tellus,* **57A,** 12–20.

——, and P. Chang, 2008: A linear stability analysis of coupled tropical Atlantic variability. *J. Climate,* **21,** 2421–2436.

Watanabe, M., and M. Kimoto, 2000: On the persistence of de-

cadal SST anomalies in the North Atlantic. *J. Climate,* **13,** 3017–3028.

Wu, Z., E. K. Schneider, and B. P. Kirtman, 2004: Causes of low frequency North Atlantic SST variability in a coupled GCM. *Geophys. Res. Lett.,* **31,** L09210, doi:10.1029/2004GL019548.

Xie, S.-P., 1999: A dynamic ocean–atmosphere model of the tropical Atlantic decadal variability. *J. Climate,* **12,** 64–70.

——, and S. G. H. Philander, 1994: A coupled ocean-atmosphere model of relevance to the ITCZ in the eastern Pacific. *Tellus,* **46A,** 340–350.

——, and J. A. Carton, 2004: Tropical Atlantic variability: Patterns, mechanisms, and impacts. *Earth Climate: The Ocean-Atmosphere Interactions, Geophys. Monogr.,* Vol. 147, Amer. Geophys. Union, 121–142.

Zebiak, S., 1993: Air–sea interaction in the equatorial Atlantic region. *J. Climate,* **6,** 1567–1586.